Bioorganic & Medicinal Chemistry Letters 22 (2012) 3873–3878

Contents lists available at SciVerse ScienceDirect

Bioorganic & Medicinal Chemistry Letters

journal homepage: www.elsevier.com/locate/bmcl

Identification, optimisation and in vivo evaluation of oxadiazole DGAT-1 inhibitors for the treatment of obesity and diabetes

William McCoull *, Matthew S. Addie, Alan M. Birch, Susan Birtles, Linda K. Buckett, Roger J. Butlin, Suzanne S. Bowker, Scott Boyd, Stephen Chapman, Robert D.M. Davies, Craig S. Donald, Clive P. Green, Chloe Jenner, Paul D. Kemmitt, Andrew G. Leach, Graeme C. Moody, Pablo Morentin Gutierrez, Nicholas J. Newcombe, Thorsten Nowak, Martin J. Packer, Alleyn T. Plowright, John Revill, Paul Schofield, Chris Sheldon, Steve Stokes, Andrew V. Turnbull, Steven J.Y. Wang, David P. Whalley, J. Matthew Wood

Cardiovascular & Gastrointestinal Innovative Medicines Unit, AstraZeneca, Alderley Park, Macclesfield, Cheshire SK10 4TG, UK

ARTICLE INFO

Article history:
Received 3 April 2012
Revised 25 April 2012
Accepted 27 April 2012
Available online 2 May 2012

Keywords:
DGAT
Oxadiazole
LLE
Obesity
PK/PD

ABSTRACT

A novel series of DGAT-1 inhibitors was discovered from an oxadiazole amide high throughput screening (HTS) hit. Optimisation of potency and ligand lipophilicity efficiency (LLE) resulted in a carboxylic acid containing clinical candidate **53** (**AZD3988**), which demonstrated excellent DGAT-1 potency (0.6 nM), good pharmacokinetics and pre-clinical in vivo efficacy that could be rationalised through a PK/PD relationship.

Inhibition of diacylglycerol acyl transferase-1 (DGAT-1) is of increasing interest as a mechanism for therapeutic treatment of diabetes, obesity and other diseases which together constitute metabolic syndrome.[1–3] DGAT-1 deficient ($Dgat^{-/-}$) mice are viable, resistant to weight gain when fed a high-fat diet and show increased insulin and leptin sensitivity.[4] Ourselves,[5] and others[6–14] have recently reported small molecule inhibitors of DGAT-1 from different chemical series and the progress of some compounds into clinical development supports the potential for therapeutic use.[15–17] In this Letter we report our discovery and optimisation of oxadiazole amide inhibitors, leading to the clinical candidate **53 (AZD3988)**.

High throughput screening (HTS) of the AstraZeneca compound collection was conducted and identified oxadiazole amide **1** (Fig. 1) originating from a kinase directed screening library (although inactive against a panel of kinases). This compound had moderate potency as a DGAT-1 inhibitor (IC_{50} = 0.52 μM)[18] and was selective against the related DGAT-2 enzyme (zero inhibition at 10 μM).[19] The log *D* was measured[20] at 3.0 resulting in an acceptable ligand lipophilicity efficiency (LLE)[21] start point of 3.2. Consequently, improvement in potency and LLE were key aims throughout the optimisation campaign.

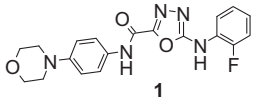

1

Figure 1. HTS hit from high throughput screening.

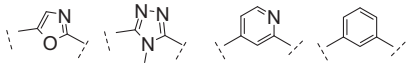

Figure 2. Unsuccessful oxadiazole replacements.

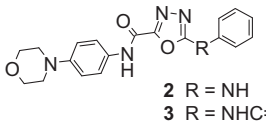

2 R = NH
3 R = NHC=O

Figure 3. Amido and anilino oxadiazole leads.

Initial chemistry efforts were focused on understanding the key features necessary for potency within the core of the molecule. The oxadiazole was systematically replaced by numerous heteroaryl and phenyl ring systems (Fig. 2) but all resulted in significant

* Corresponding author.
E-mail address: william.mccoull@astrazeneca.com (W. McCoull).

0960-894X/$ - see front matter © 2012 Elsevier Ltd. All rights reserved.
http://dx.doi.org/10.1016/j.bmcl.2012.04.117

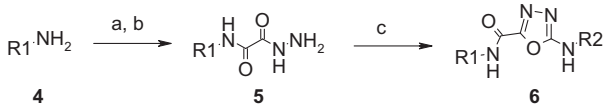

Scheme 1. General synthetic procedure for substituted oxadiazole amides. Reagents: (a) MeOCOCOCl, pyridine, CH_2Cl_2; (b) NH_2NH_2, EtOH, reflux; (c) R_2NCS, PS-CDI.

potency loss (>10-fold). Similarly, methylation of either the amide or aniline nitrogen resulted in loss of potency. The pharmacophore was not tolerant to changes anywhere but the terminal fragments.

The only encouraging alteration to the amide-oxadiazole-aniline core was conversion of the aniline **2** (IC_{50} = 0.30 μM, LLE = 3.4) to an amide **3** (IC_{50} = 5.2 μM, LLE = 4.3) as shown in Figure 3. Although potency was reduced, the bis-amide compound **3** showed improved LLE and both these sub-series were progressed to lead expansion activities.

The compounds described in this Letter were prepared using similar methods[22,23] which allowed diversification of R1 and R2 (Scheme 1). Starting with anilines **4**, reaction with methyl chlorooxoacetate followed by hydrazine afforded acyl-hydrazines **5** which were condensed with various isothiocyanates. Ring closure to form oxadiazoles **6** was effected using polymer-supported carbodiimide (PS-CDI)

The amide-oxadiazole-aniline sub-series was initially explored as a two-dimensional array, varying R1 and R2. Principal component analysis[24], using common descriptors such as *c*log*P*, polar surface area (PSA) and hydrogen bond counts, was used to guide design of a diverse set of compounds but all significant structural deviations away from **1** resulted in a loss of potency (data not shown). Consequently, more conservative SAR exploration was conducted around the morpholino aryl side chain R1 (Table 1). Addition of a single F (**7**) or Me (**8**) group on the arylamide-3-position maintained potency but with lower LLE. However, at the arylamide-2-position F (**9**) resulted in a loss of potency. Lowering lipophilicity by conversion of the aryl group to a pyridine could be tolerated with the 3-aza **10** improving potency whereas the 2-aza compound **11** showed a significant decrease. Changing the morpholine to more lipophilic groups, for example piperidine **12** or thiomorpholine **13**, also improved potency. Although potent, **13** exhibited high in vitro clearance in human microsomes (Cl_{int} = 258 μL/min/mg) and low oral exposure in rat (C_{max} = 0.02 μM from 2 mg/kg dose) thus was not progressed. Oxidation of **13** to sulfoxide **14** reduced potency. Piperazines **15** and **16** were both tolerated and gave improved LLE. Low aqueous solubility, typically less than 10 μM was a problematic feature for all these analogues which were generally synthesized in a crystalline form. Basic compound **15** did show higher solubility of 91 μM but high clearance in rat of greater than 100% liver blood flow precluded further optimisation of such compounds.

Increasing flexibility through introducing sp^3 character was used as a tactic to improve solubility and explore SAR (Table 2). Unfortunately, solubility remained low although carbon, oxygen, nitrogen or sulfur could be used as a linker with a suitably large substituent to achieve good potency. Notably, increasingly lipophilic ethers such as compounds **20**–**22**, gave increasing potency suggesting a lipophilic binding interaction was responsible. Reduced potency of pyridine **23** is consistent with this hypothesis. Lipophilicity was generally too high to be accurately measured, only **20** and **23** returning log *D* values of 3.2 and 3.1 respectively, thus further exploration to achieve our dual potency and LLE aims was not justified

The aniline R2 group was extensively explored and a large variety of substitution was tolerated at several positions on the aryl ring (Table 3). Notably, substitution at the 3-position often gave

Table 1
DGAT-1 potency, log *D* and LLE for selected R1 variations

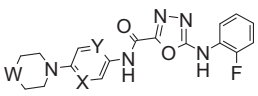

Compd	X	Y	W	h DGAT-1 IC_{50}[a] (μM)	log *D*	LLE
1	CH	CH	O	0.52	3.0	3.2
7	CF	CH	O	0.46	3.6	2.7
8	CMe	CH	O	0.35	4.0	2.5
9	H	CF	O	>30	3.4	—
10	N	CH	O	0.13	2.7	4.2
11	CH	N	O	11	2.4	2.5
12	CH	CH	CH_2	0.19	>4.2	—
13	N	CH	S	0.023	3.0	4.6
14	N	CH	S=O	3.7	—	—
15	N	CH	NM e	0.46	2.4	4.0
16	CH	CH	NHAc	0.54	2.5	3.8

[a] Mean values from ⩾2 experiments.

Table 2
DGAT-1 potency for selected morpholine replacements

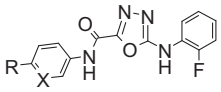

Compd	X	R	h DGAT-1 IC_{50}[a] (μM)
10	N	Morpholine	0.13
17	CH	*n*-Bu	0.62[b]
18	CH	c-Hex	0.31
19	CH	Ph	0.12
20	N	MeO	8.0
21	N	*n*-BuO	0.060
22	N	PhO	0.0067
23	N	3-PyridylO	0.41
24	N	PhN	0.060
25	CH	*n*-BuS	0.016

[a] Mean values from ⩾2 experiments unless otherwise stated.
[b] *n* = 1.

Table 3
DGAT-1 potency, log *D* and LLE for selected R2 variations

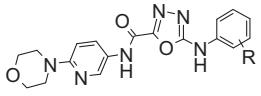

Compd	R	h DGAT-1 IC_{50}[a] (μM)	log *D*	LLE
26	H	0.62	2.9	3.3
10	2-F	0.13	2.7	4.2
27	3-F	0.15	3.2	3.6
28	4-F	0.84	3.0	3.1
29	3,4-diF	0.34	2.9	3.6
30	2-Cl	1.3[b]	2.9	3.0
31	3-Cl	0.092	>3.4	—
32	4-Cl	0.19	—	—
33	3-OMe	0.73[b]	2.8	3.3
34	3-OEt	0.032[b]	3.6	3.9
35	3-OPh	0.0066[b]	>4.2	—
36	3-OCH_2Ph	0.013	>4.2	—
37	3-OCH_2-2-pyridyl	0.54	3.1	3.2
38	3-OCH_2-3-pyridyl	2.1	3.3	2.4
39	3-Me	0.17	3.4	3.4
40	3-Ph	0.0057	>4.0	—
41	3-CO_2H	>30[b]	—	—

[a] Mean values from ⩾2 experiments unless otherwise stated.
[b] *n* = 1.

increased potency. Increasing lipophilic bulk at this position gave increasing potency within an ether series (compounds **33–36**) and again attempts to introduce polarity generally resulted in a loss of potency, for example compounds **37** and **38**. Introduction of a carboxylic acid was not well tolerated in compound **41**.

The bis-amide sub-series afforded the opportunity to achieve higher solubility by means of an ionisable centre. The pKa of such compounds was typically in the range 5–7, depending on other substituents and resulted in solubilities generally greater than 10 μM. Modest DGAT -1 potency improvements could be made but were generally accompanied with increased lipophilicity and decreased LLE (Table 4). High metabolic clearance, particularly in rat (e.g., **43** showed 62% liver blood flow and 3% bioavailability), led us to discontinue work in this series.

Introduction of an ionisable centre, particularly a carboxylic acid remained a key goal to obtain acceptable solubility and high LLE. Disclosure of a potent acidic series in the patent literature[25] encouraged us to continue to explore the incorporation of an acid group into the R1 side chain (Table 5). Modestly potent butanoate **46** indicated that this would be possible and biphenyl containing acids **47–49** maintained potency relative to the biphenyl non-acid

Table 4
DGAT-1 potency, log *D* and LLE for selected bis-amides

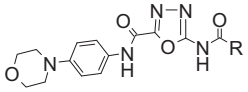

Compd	R	h DGAT-1 IC_{50}[a] (μM)	log *D*	LLE
42	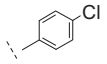	0.37	1.9	4.5
43	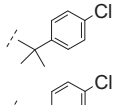	0.52	3.0	3.3
44	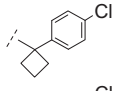	0.32	3.2	3.3
45	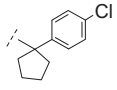	0.18	3.7	3.0

[a] Mean values from ⩾2 experiments.

Table 5
DGAT-1 potency, log *D* and LLE for selected acids

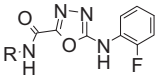

Compd	R	h DGAT-1 IC_{50}[a] (μM)	log *D*	LLE
46	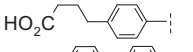	3.3[b]	–	–
47	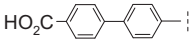	0.21[b]	–	–
48	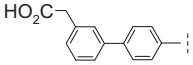	0.07	–	–
49	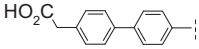	0.08	1.5	5.6
50	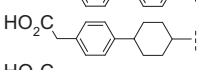	1.3	–	–
51	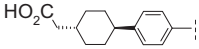	0.0044	2.4	5.9
52	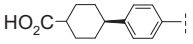	0.035	2.1	5.4

[a] Mean values from ⩾2 experiments unless otherwise stated.
[b] $n = 1$.

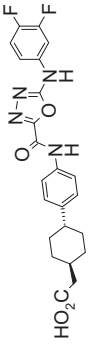

53

Table 6
Selected properties for **53**

h DGAT-1 IC_{50} (μM)	Rat DGAT-1 IC_{50} (μM)	Mouse DGAT-1 IC_{50} (μM)	HuTu 80 cell IC_{50}[a] (μM)	h DGAT-2 %inhib @ 10 μM	log *D*	LLE	aq solubility pH 7.4 (μM)	h/rat plasma protein binding (%free)	MDCK permeability P_{app}[b] ($\times 10^{-6}$cm s^{-1})
0.0006	0.0005	0.0011	0.0005	12	3.0	6.2	2.1	0.3/0.08	12 (A–B), 14 (B–A)

[a] Inhibition of triacylglycerol synthesis in HuTu 80 cells.
[b] Compounds were incubated at 10 μM in cultured Madin–Darby canine kidney (MDCK) cells and permeability was measured in both the A to B and B to A directions

Table 7
Pharmacokinetic parameters for **53**[a]

Species	Clp (mL/min/kg)	V_{dss} (L/kg)	IV half-life (h)	po half-life (h)	po C_{max} (μM)	Bioavailability (%)
Mouse	4.6	0.99	4.9	4.7	1.9	>100
Rat	1.1	0.35	3.4	5.8	20	>100
Dog	2.5	0.36	1.8	5.7	1.5	32

[a] Compound was dosed IV at 0.5 mg/kg (mouse), 2 mg/kg (rat) and 1 mg/kg (dog) and po at 1 mg/kg (mouse) in 5% DMSO: 95% hydroxypropyl β cyclodextrin; po at 5 mg/kg (rat) and 1 mg/kg (dog) in hydroxypropyl methylcellulose (HPMC) with 0.1% polysorbate.

19. Saturation of either ring resulted in decreased potency in **50** but significantly increased potency in **51** relative to the non-acid **18**. Subsequent to this work, the acid fragment R in **51** has been reported as a privileged structure contained within several DGAT-1 inhibitors.[5,12,13,26] Des-homologue **52** was also potent but the phenyl-*c*-hexyl-ethanoate group gave a clear potency and LLE advantage.

Our previous R2 aniline SAR could be mapped onto a new acid-containing sub-series and **53 (AZD3988)** was quickly identified as having a good overall balance of properties, most notably achieving our key aims of high potency and LLE (Table 6). Excellent potency in inhibiting triacylglycerol (TAG) synthesis in human HuTu 80 cells, relevant to the gut as a target organ, was determined. **53** showed no significant activity against DGAT-2, the hERG encoded potassium channel (>30 μM), and cytochrome P450 enzymes CYP1A2, CYP2C9, CYP2C19, CYP2D6 and CYP3A4 (all >30 μM). Aqueous solubility of crystalline **53** is lower than ideal but is counterbalanced by good cellular permeability, resulting in good pharmacokinetic profiles determined in vivo in three pre-clinical species: mouse, rat and dog (Table 7). Oral exposure was substantial in all species. The rat and mouse pharmacokinetic profiles were characterised by high oral bioavailability and low clearance while more moderate bioavailability was observed in dog.

In an oral lipid tolerance test (OLTT), fasted rats were administered compound **53** at a range of doses 2 h prior to a bolus dose of corn oil and plasma TAG levels were measured 1.5 h later. Figure 4a shows that **53** was highly efficacious in reducing plasma TAG

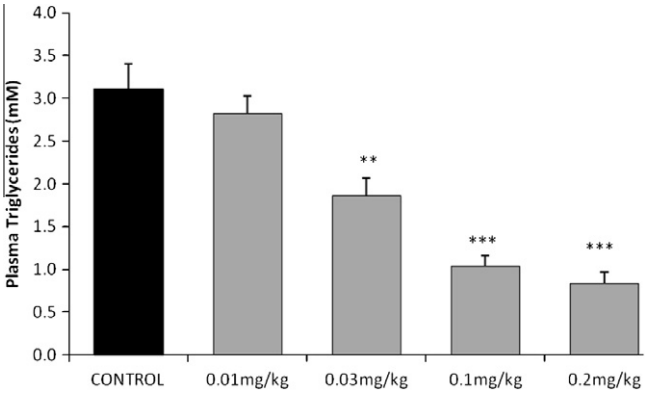

Figure 4a. Pharmacodynamic effects of **53**. Dose related reduction in plasma TAG excursion at 1.5 h post bolus corn oil administration. Mean values ± SEM (**p <0.01, ***p <0.001).

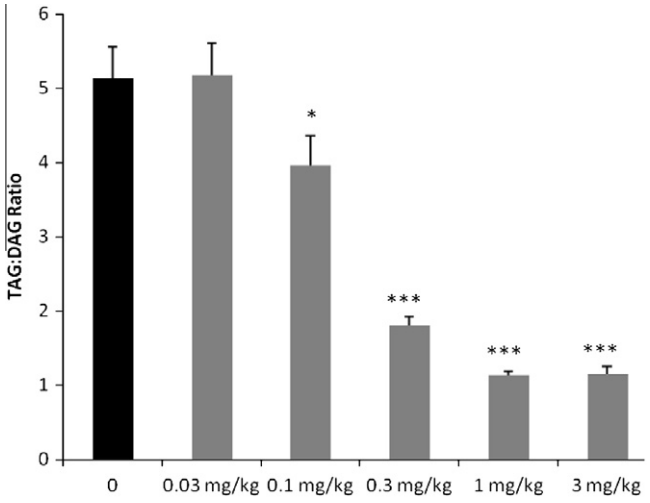

Figure 5a. Pharmacodynamic effects of **53**. Dose related reduction in adipose triacylglycerol synthesis as determined by changes in the ratio of radiolabel incorporation into TAG and DAG. Mean values ± SEM (*p <0.05, ***p <0.001).

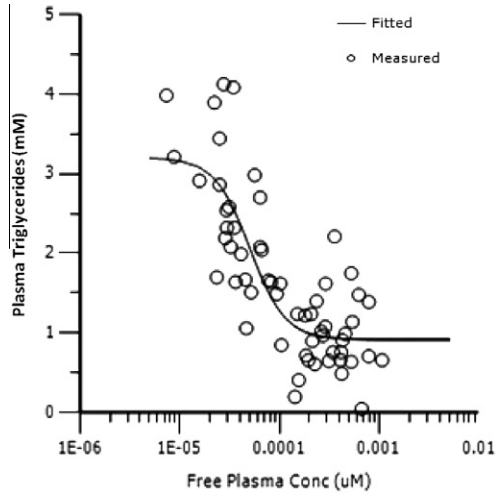

Figure 4b. PK/PD analysis of rat OLTT (plasma TAG vs free compound concentrations in plasma) for **53**. A direct response (E_{max} sigmoidal) model was used to fit the PK/PD data.

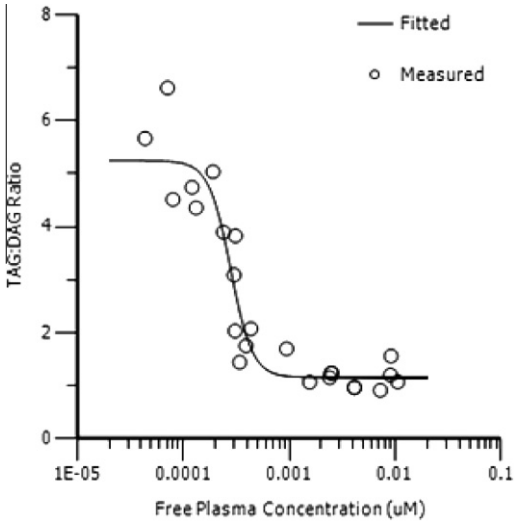

Figure 5b. PK/PD analysis of rat adipose TAG synthesis assay (adipose tissue TAG:DAG ratio vs free compound concentrations in plasma) for **53**. A direct response (E_{max} sigmoidal) model was used to fit the PK/PD data.

Table 8
PK/PD parameters for model fit for **53** in the rat OLTT

Parameter	Estimate	Units	Stderr%
IC_{50}	0.00005	μM	17
Gamma	2.4	–	30
E0	3.2	mM	6.8
I_{max}	2.3	mM	11

excursion in this model, exhibiting 40%, 66% and 73% inhibition at doses of 0.03, 0.1 and 0.2 mg/kg respectively. Fig. 4b shows the relationship between plasma TAG and free compound levels in plasma for **53** in the rat OLTT assay. A direct response PK/PD model (E_{max} sigmoidal model) was used to successfully fit the PK/PD data showing a clear correlation between compound levels in plasma and an effect in the OLTT. PK/PD parameters for the model fit are shown in Table 8. The fact that the in vivo IC_{50} (0.00005 μM) is 10-fold lower than the in vitro IC_{50} (0.0005 μM) is compatible with the idea that local inhibition of DGAT-1 in the gut (and not the systemic exposure) could be the main driver for efficacy in the OLTT assay.

$$E = E0 - \frac{I_{max} \times C^{\gamma}}{IC_{50}^{\gamma} + C^{\gamma}}$$

Compound **53** also showed good effects on adipose TAG synthesis (expressed as TAG:DAG ratio in adipose tissue) giving 33%, 65%, 78% and 78% decrease in the TAG:DAG ratio in adipose tissue at 0.1, 0.3, 1 and 3 mg/kg, respectively (Fig. 5a). Fig. 5b shows the relationship between adipose TAG synthesis and free compound levels in plasma for **53** in the rat. A direct response PK/PD model (E_{max} sigmoidal model) was used to succesfully fit the PK/PD data showing a clear correlation between free compound levels in plasma and an effect in the adipose TAG:DAG ratio. PK/PD parameters for the model fit are shown on Table 9.

The in vivo IC_{50} (0.0003 μM) in the adipose tissue assay is in very good agreement with the in vitro IC_{50} (0.0005 μM), and it is larger than the one measured in the OLTT assay (0.00005 μM) for this compound. These differences in in vivo IC_{50} between OLTT and TAG synthesis are expected as we used free compound concentration in plasma as a surrogate for compound concentration at the target. In the OLTT assay we believe that local compound concentrations in the gut are driving effects and therefore using systemic exposure as a surrogate will underestimate the compound concentrations at the target leading to a smaller IC_{50}. For the adipose TAG synthesis assay that does not seem to be the case and the observed in vivo IC_{50} using free compound concentration in plasma is in very good agreement with the in vitro one.

$$E = E0 - \frac{I_{max} \times C^{\gamma}}{IC_{50}^{\gamma} + C^{\gamma}}$$

To assess the activity in a model of diet-induced obesity (DIO), **53** was tested for effects on body weight loss in DIO mice (Fig. 6). Treatment for 3 days resulted in a statistically significant reduction in body weight compared to start weight and in comparison with age-matched vehicle treated control mice on the same diet. In

Table 9
PK/PD parameters for model fit for **53** in the rat adipose TAG synthesis assay

Parameter	Estimate	Units	Stderr%
IC_{50}	0.0003	μM	7.8
Gamma	4.2	–	42
E0	5.2	–	4.9
I_{max}	4.1	–	7.1

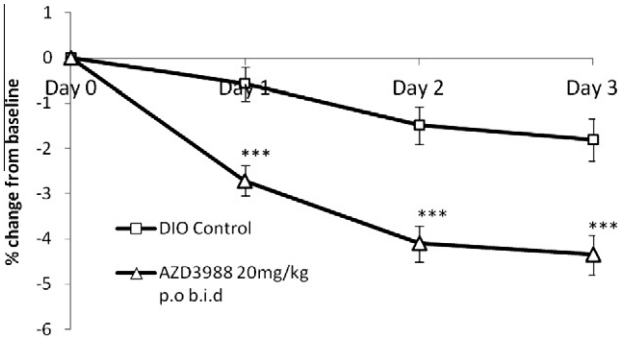

Figure 6. Percentage reduction in body weight compared to start weight in DIO mice receiving high energy cafeteria diet. Day 0 is first treatment day; mice weighed and dosed at 6:00 and 16:00 each day. In mice receiving **53**, statistical differences from DIO controls were seen at all time points (***p <0.001).

the mouse DIO study for **53**, free compound concentrations in plasma were maintained >20-fold above the in vitro IC_{50} (0.0011 μM) for the whole dosing interval. At these compound concentrations, based on the rat PK/PD knowledge, it is expected that compound **53** has fully inhibited DGAT-1 both in the gut and in the adipose tissue. These effects on body weight appear specific and consistent with the mechanism of action. Accordingly **53** had no effects on body weight at similar or even higher exposures in lean animals, and effects on food intake were only observed in animals fed a high fat diet.

In summary, the novel oxadiazole DGAT-1 inhibitor **1** was identified and SAR exploitation enabled a design strategy to improve both potency and LLE leading to the clinical candidate **53 (AZD3988)**, which displayed good pharmacokinetics and demonstrated in vivo efficacy in obesity related models. Results from the further development of **53 (AZD3988)** as a drug to treat metabolic disease will be reported in due course.

Acknowledgments

Teresa Collins and Mark Denn are acknowledged for expert technical assistance in generating DMPK data. Usha Chauhan's expert technical assistance in generating enzyme inhibition data is also acknowledged.

References and notes

1. Zammit, V. A.; Buckett, L. K.; Turnbull, A. V.; Wure, H.; Proven, A. *Pharmacol. Ther.* **2008**, *118*, 295.
2. Hubbard, B. K.; Enyedy, I.; Gilmore, T. A.; Serrano-Wu, M. *Expert Opin. Ther. Pat.* **2007**, *17*, 1331.
3. Matsuda, D.; Tomoda, H. *Curr. Opin. Invest. Drugs (Thomson Sci.)* **2007**, *8*, 836.
4. Chen, H. C.; Farese, R. V. *Arterioscler., Thromb., Vasc. Biol.* **2005**, *25*, 482.
5. Birch, A. M.; Birtles, S.; Buckett, L. K.; Kemmitt, P. D.; Smith, G. J.; Smith, T. J. D.; Turnbull, A. V.; Wang, S. J. Y. *J. Med. Chem.* **2009**, *52*, 1558.
6. Zhao, G.; Souers, A. J.; Voorbach, M.; Falls, H. D.; Droz, B.; Brodjian, S.; Lau, Y. Y.; Iyengar, R. R.; Gao, J.; Judd, A. S.; Wagaw, S. H.; Ravn, M. M.; Engstrom, K. M.; Lynch, J. K.; Mulhern, M. M.; Freeman, J.; Dayton, B. D.; Wang, X.; Grihalde, N.; Fry, D.; Beno, D. W. A.; Marsh, K. C.; Su, Z.; Diaz, G. J.; Collins, C. A.; Sham, H.; Reilly, R. M.; Brune, M. E.; Kym, P. R. *J. Med. Chem.* **2008**, *51*, 380.
7. Nakada, Y.; Aicher, T. D.; Huerou, Y. L.; Turner, T.; Pratt, S. A.; Gonzales, S. S.; Boyd, S. A.; Miki, H.; Yamamoto, T.; Yamaguchi, H.; Kato, K.; Kitamura, S. *Bioorg. Med. Chem.* **2010**, *18*, 2785.
8. Qian, Y.; Wertheimer, S. J.; Ahmad, M.; Cheung, A. W.; Firooznia, F.; Hamilton, M. M.; Hayden, S.; Li, S.; Marcopulos, N.; McDermott, L.; Tan, J.; Yun, W.; Guo, L.; Pamidimukkala, A.; Chen, Y.; Huang, K.; Ramsey, G. B.; Whittard, T.; Conde-Knape, K.; Taub, R.; Rondinone, C. M.; Tilley, J.; Bolin, D. *J. Med. Chem.* **2011**, *54*, 2433.
9. Yun, W.; Ahmad, M.; Chen, Y.; Gillespie, P.; Conde-Knape, K.; Kazmer, S.; Li, S.; Qian, Y.; Taub, R.; Wertheimer, S. J.; Whittard, T.; Bolin, D. *Bioorg. Med. Chem. Lett.* **2011**, *21*, 7205.
10. Fox, B. M.; Iio, K.; Li, K.; Choi, R.; Inaba, T.; Jackson, S.; Sagawa, S.; Shan, B.; Tanaka, M.; Yoshida, A.; Kayser, F. *Bioorg. Med. Chem. Lett.* **2010**, *20*, 6030.
11. Motiwala, H.; Kandre, S.; Birar, V.; Kadam, K. S.; Rodge, A.; Jadhav, R. D.; Mahesh Kumar Reddy, M.; Brahma, M. K.; Deshmukh, N. J.; Dixit, A.; Doshi, L.;

Gupte, A.; Gangopadhyay, A. K.; Vishwakarma, R. A.; Srinivasan, S.; Sharma, M.; Nemmani, K. V. S.; Sharma, R. *Bioorg. Med. Chem. Lett.* **2011**, *21*, 5812.
12. Dow, R. L.; Li, J.; Pence, M. P.; Gibbs, E. M.; LaPerle, J. L.; Litchfield, J.; Piotrowski, D. W.; Munchhof, M. J.; Manion, T. B.; Zavadoski, W. J.; Walker, G. S.; McPherson, R. K.; Tapley, S.; Sugarman, E.; Guzman-Perez, A.; DaSilva-Jardine, P. *ACS Med. Chem. Lett.* **2011**, *2*, 407.
13. Dow, R. L.; Andrews, M.; Aspnes, G. E.; Balan, G.; Michael Gibbs, E.; Guzman-Perez, A.; Karki, K.; LaPerle, J. L.; Li, J.; Litchfield, J.; Munchhof, M. J.; Perreault, C.; Patel, L. *Bioorg. Med. Chem. Lett.* **2011**, *21*, 6122.
14. Bali, U.; Barba, O.; Dawson, G.; Gattrell, W. T.; Horswill, J. G.; Pan, D. A.; Procter, M. J.; Rasamison, C. M.; Sambrook Smith, C. P.; Taylor-Warne, A.; Wong-Kai-In, P. *Bioorg. Med. Chem. Lett.* **2012**, *22*, 824.
15. Birch, A. M.; Buckett, L. K.; Turnbull, A. V. *Curr. Opin. Drug Discov. Devel.* **2010**, *13*, 489.
16. King, A. J.; Judd, A. S.; Souers, A. J. *Expert Opin. Ther. Pat.* **2010**, *20*, 19.
17. Cao, J.; Zhou, Y.; Peng, H.; Huang, X.; Stahler, S.; Suri, V.; Qadri, A.; Gareski, T.; Jones, J.; Hahm, S.; Perreault, M.; McKew, J.; Shi, M.; Xu, X.; Tobin, J. F.; Gimeno, R. E. *J. Biol. Chem.* **2011**, *286*, 41838.
18. Assay protocols can be found in Ref. 5
19. Lardizabal, K. D.; Mai, J. T.; Wagner, N. W.; Wyrick, A.; Voelker, T.; Hawkins, D. J. *J. Biol. Chem.* **2001**, *276*, 38862.
20. Buttar, D.; Colclough, N.; Gerhardt, S.; MacFaul, P. A.; Phillips, S. D.; Plowright, A.; Whittamore, P.; Tam, K.; Maskos, K.; Steinbacher, S.; Steuber, H. *Bioorg. Med. Chem.* **2010**, *18*, 7486.
21. Leeson, P. D.; Springthorpe, B. *Nat. Rev. Drug Discov.* **2007**, *6*, 881.
22. Birch, A. M.; Bowker, S. S.; Butlin, R. J.; Donald, C. S.; McCoull, W.; Nowak, T.; Plowright, A. *PCT Int. Appl.* **2006**, 418.
23. Butlin, R. J.; Green, C. P.; McCoull, W. *PCT Int. Appl.* **2006**, 74.
24. Wold, S.; Geladi, P.; Esbensen, K.; Oehman, J. *J. Chemom.* **1987**, *1*, 41.
25. Fox, B. M.; Furukawa, N.; Hao, X.; Iio, K.; Inaba, T.; Jackson, S. M.; Kayser, F.; Labelle, M.; Li, K.; Matsui, T.; McMinn, D. L.; Ogawa, N.; Rubenstein, S. M.; Sagawa, S.; Sugimoto, K.; Suzuki, M.; Tanaka, M.; Ye, G.; Yoshida, A.; Zhang, J. *PCT Int. Appl.* **2004**, 176.
26. Yeh, V. S. C.; Beno, D. W. A.; Brodjian, S.; Brune, M. E.; Cullen, S. C.; Dayton, B. D.; Dhaon, M. K.; Falls, H. D.; Gao, J.; Grihalde, N.; Hajduk, P.; Hansen, T. M.; Judd, A. S.; King, A. J.; Klix, R. C.; Larson, K. J.; Lau, Y. Y.; Marsh, K. C.; Mittelstadt, S. W.; Plata, D.; Rozema, M. J.; Segreti, J. A.; Stoner, E. J.; Voorbach, M. J.; Wang, X.; Xin, X.; Zhao, G.; Collins, C. A.; Cox, B. F.; Reilly, R. M.; Kym, P. R.; Souers, A. J. *J. Med. Chem.* **2012**, *55*, 1751.